Chinese Journal of Electronics
vol. 33, no. 5, pp. 1253–1260, September 2024
https://doi.org/10.23919/cje.2022.00.410

RESEARCH ARTICLE

A Polarization Control Operator for Polarized Electromagnetic Wave Designing

Shuo CUI[1,2], Yaoyao LI[3], Shijian ZHANG[3], Ling CHEN[3], Cheng CAO[3], and Donglin SU[1,3]

1. *School of Electronic and Information Engineering, Beihang University, Beijing 100083, China*
2. *Shenyuan Honors College, Beihang University, Beijing 100083, China*
3. *Research Institute for Frontier Science, Beihang University, Beijing 100083, China*

Corresponding author: Yaoyao LI, Email: liyaoyao@buaa.edu.cn
Manuscript Received November 29, 2022; Accepted December 21, 2022

Abstract — To describe and control the polarization state of electromagnetic waves, a polarization control operator of the complex vector form is proposed. Distinct from traditional descriptors, the proposed operator employs an angle parameter to configure the polarization state of the polarized wave. By setting the parameter in the proposed operator, the amplitude of the field components can be modified, resulting in changes in the magnitude and direction of the field vector, and thus realizing control of the polarization state of the electromagnetic wave. The physical meaning, orthogonal decomposition, and discrete property of the proposed operator are demonstrated through mathematical derivation. In the simulation examples, the polarization control operator with fixed and time-varying parameters is applied to the circularly polarized wave. The propagation waveform, the trajectory projection and the waveform cross section in different reception directions of the new electromagnetic waves are observed. The simulation results indicate that complex electromagnetic waves with more flexible polarization states can be obtained with the aid of the polarization operator.

Keywords — Electromagnetic wave, Polarization control operator, Polarization descriptor, Polarization state.
Citation — Shuo CUI, Yaoyao LI, Shijian ZHANG, *et al.*, "A Polarization Control Operator for Polarized Electromagnetic Wave Designing," *Chinese Journal of Electronics*, vol. 33, no. 5, pp. 1253–1260, 2024. doi: 10.23919/cje.2022.00.410.

I. Introduction

The polarization properties of electromagnetic waves have enhanced the development of many fields. In the field of communication, the electromagnetic spectrum resources are limited. The new dimension introduced by polarization allows the spectrum resources to be extended [1]–[3]. In the field of target identification, the material and geometry of the targets are reflected in the polarized scattering characteristics. The polarization domain can provide more characteristic information about the targets [4], [5]. Therefore, the study of polarization control of electromagnetic waves is important.

Polarization is first investigated in the field of optics. The polarization ellipse method provides a good physical understanding of elliptically polarized waves, but it is not convenient mathematically [6]. In 1941, Jones found that the polarized light could be represented by the Jones vector [7] and the polarization state of the light transmitted through a polarization device can be analyzed with the vector. The Jones matrix is convenient in mathematics but is restricted to describe the fully polarized electromagnetic waves [8], [9]. Stokes introduced four quantities to characterize the amplitude and polarization of a light wave [10]. This description can be used to describe the optical field with arbitrary polarization properties and forms the basis of modern polarization measurement. In 1892, the Poincaré sphere was proposed to describe arbitrary polarization states [11]. By stereographic projection, a one-to-one correspondence between arbitrary polarization and point on the sphere is established. After normalization, the Poincaré sphere can directly characterize arbitrary polarization states, including natural light, partially polarized light, and fully polarized light, and is a very intuitive and convenient way to represent polarization states [12], [13].

Along with the polarization domain being widely studied, its application prospects are broadened. Some

Associate Editor: Prof. Chao-Hai DU, Peking University.

researchers work on designing communication systems with a special polarization state. A high-gain dual circularly polarized antenna is presented in [14] for E-band air-to-ground wireless link. A double V-shaped metasurface is proposed in [15] to efficiently convert linear polarizations of electromagnetic waves in wideband. A digital communication system is developed in [16] by exploiting circular polarization of the propagating electromagnetic carrier as a modulation attribute. Further, the multi-polarization system is designed to transmit high-speed signals [17]–[19]. A novel polarization-reconfigurable microstrip antenna with a simple structure is presented in [20] to match modern wireless system requirements with a cost-effective solution. A polarization-reconfigurable antenna is designed in [21] to realize high gains for 5G communication applications. Recently, orbital angular momentum (OAM) was introduced into wireless communication system design [22]–[24]. The orthogonal modes of OAM increase the channel capacity without extra frequency bands.

Still, in order to further develop the potential of polarize domain, a polarization description method with both clear geometric meaning and mathematical simplicity is expected. In this paper, a novel polarization control operator is proposed. The polarization state of electromagnetic waves can be described with the proposed operator, and the polarization state of electromagnetic waves can be designed by assigning values to the characteristic parameter of the proposed operator.

The rest of this paper is organized as follows. In Section II, the polarization operator is derived in detail and analyzed in terms of implication, orthogonal decomposition characteristic, and discrete sequences form. Section III gives simulation results of the polarized electromagnetic waves controlled by the proposed operator with constant and time-varying parameters. The polarization state of the wave is changed to different constant polarization states and complex time-varying polarization states, respectively. Finally, Section IV draws a brief conclusion. Appendix A lists the mathematical transformation formulas of the proposed operator.

II. Formulation of the Polarization Control Operator

First, this section demonstrates the definition of the polarization control operator and how it re-expresses the instantaneous field of any general harmonic waves. Then, the implication of the proposed operator is analyzed to show how it controls the polarization state of the instantaneous cross section of the electromagnetic wave. Finally, in order to make the operator more practical, the orthogonal decomposition and discrete sequence forms of the operator are derived.

1. Definition of the polarization control operator

The instantaneous field of a single-frequency wave propagating along $\boldsymbol{w}$ can be generally written as [25]

$$\boldsymbol{E} = \boldsymbol{u}a_u\cos(\omega t - g_u) + \boldsymbol{v}a_v\cos(\omega t - g_v) \tag{1}$$

where $\boldsymbol{u}$ and $\boldsymbol{v}$ are orthogonal unit vectors on the plane perpendicular to the propagation direction, a_u and a_v are real amplitude of the field components, g_u and g_v and real spatial phase of the field components. If we define a coefficient:

$$c = -\frac{\cos(\omega t - g_v)}{\sin(\omega t - g_u)}$$

and let

$$\cos\alpha = a_u/A$$

$$\sin\alpha = ca_v/A$$

where $A = \sqrt{a_u^2 + (ca_v)^2}$. Then equation (1) can be transformed to

$$\boldsymbol{E} = A[\boldsymbol{u}\cos\alpha\cos(\omega t - g_u) - \boldsymbol{v}\sin\alpha\sin(\omega t - g_u)] \tag{2}$$

To separate the "wave" properties and the "polarization" properties of the field, equation (2) is decomposed as

$$\begin{aligned}\boldsymbol{E} =& \mathrm{Re}[A(\cos(\omega t - g_u) + \mathrm{j}\sin(\omega t - g_u))(\boldsymbol{u}\cos\alpha \\ &+ \mathrm{j}\boldsymbol{v}\sin\alpha)]\end{aligned} \tag{3}$$

where Re[ ] is the real-part operator. We define a complex vector:

$$\mathbf{rot}\alpha = \boldsymbol{u}\cos\alpha + \mathrm{j}\boldsymbol{v}\sin\alpha$$

and name **rot**[ ] "the polarization control operator". Then the harmonic vector field of (3) can be written as

$$\boldsymbol{E} = A\mathrm{Re}[\mathrm{e}^{\mathrm{j}(\omega t - g_u)}\mathbf{rot}\alpha] \tag{4}$$

From (4), it can be found that the complex vector field $\boldsymbol{E}$ is decomposed into a complex scalar component, $A\exp[\mathrm{j}(\omega t - g_u)]$, and a complex vector component, $\mathbf{rot}\alpha$. The value of α and its variation will influence the trace of $\boldsymbol{E}$ by the polarization state of $\boldsymbol{E}$ by affecting $\boldsymbol{E}_u$ and $\boldsymbol{E}_v$.

For example, the normalized plane wave propagating along $\boldsymbol{z}$ with the polarization operator of $\alpha = 0$ represents a linearly polarized wave and is expressed as

$$\boldsymbol{E} = \mathrm{Re}[\mathrm{e}^{\mathrm{j}(\omega t - kz)}\mathbf{rot}(0)] = \boldsymbol{u}\cos(\omega t - kz)$$

When $\alpha = \pi/4$, the normalized plane wave represents a left-circularly polarized wave and is expressed as

$$\begin{aligned}\boldsymbol{E} &= \mathrm{Re}\left[\mathrm{e}^{\mathrm{j}(\omega t - kz)}\mathbf{rot}\left(\frac{\pi}{4}\right)\right] \\ &= \frac{\sqrt{2}}{2}[\boldsymbol{u}\cos(\omega t - kz) - \boldsymbol{v}\sin(\omega t - kz)]\end{aligned}$$

The following contents will show more detail about

controlling polarized electromagnetic waves with the polarization control operator.

2. Implication of the polarization control operator

According to (2), $\boldsymbol{E}_u$ is in the range of $[-|A\cos\alpha|, |A\cos\alpha|]$ and $\boldsymbol{E}_v$ is in the range of $[-|A\sin\alpha|, |A\sin\alpha|]$. Therefore, the instantaneous polarization ellipse of (4) at $t = t_0$ and $\alpha = \alpha_0$ can be bounded by the rectangle whose dimensions are $|2A\cos\alpha_0|$ and $|2A\sin\alpha_0|$, and sides are parallel to the $\boldsymbol{u}$ and $\boldsymbol{v}$ axes. The circumcircle of the rectangle has a radius of A. The tilt angle of the polarization ellipse satisfies [6]

$$\tan(2\tau_0) = 0$$

The shape and pose of a polarization ellipse can be determined by the bounding rectangle and the tilt angle. Therefore, for fields of same A values and different α values, the polarization ellipses have different title angles and different bounding rectangles in a same circumcircle, as shown in Figures 1(a)–(c).

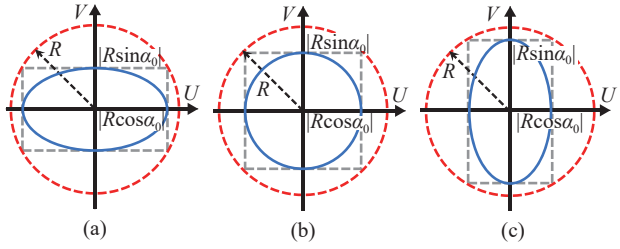

Figure 1 Polarization ellipses when α_0 takes different values in the wave expressed with the proposed polarization control operator in the UOV coordinates. (a) $\alpha_0 = \pi/6$; (b) $\alpha_0 = \pi/4$; (c) $\alpha_0 = \pi/3$.

Overall, the relation between the value of α_0 and the corresponding polarization state for waves propagating along $\boldsymbol{w}$ is symmetric, as shown in Figure 2. For the polarization pattern, when $\alpha_0 \in \{0, \pi\}$, the wave is linear horizontal; when $\alpha_0 \in \{\pi/2, 3\pi/2\}$, the wave is linear vertical; when $\alpha_0 \in \{1\pi/4, 3\pi/4, 5\pi/4, 7\pi/4\}$, the wave is circular; when α_0 takes other values, the wave is elliptical. For the rotation sense, when $\alpha_0 \in (0, \pi/2) \cup (\pi, 3\pi/2)$, the wave is left-handed; when $\alpha_0 \in (\pi/2, \pi) \cup (3\pi/2, 2\pi)$, the wave is right-handed.

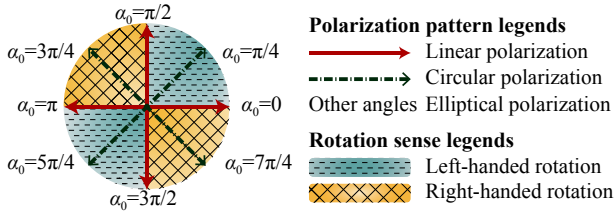

Figure 2 Relationship between the value of α_0 and the corresponding polarization state for waves propagating along $\boldsymbol{w}$.

3. Orthogonal decomposition of the polarization control operator

According to the electromagnetic field theory, a polarized plane wave can be decomposed into two plane waves of linearly independent polarization states [25]. This subsection will show that the decomposition can also be realized for the proposed polarization control operator. The decomposition of the polarization operator may be considered as an operation on the wave in the polarization domain.

We take any local orthogonal basis noted by $\boldsymbol{p}$ and $\boldsymbol{q}$ on the plane perpendicular to the propagation direction, as shown in Figure 3. Here, $(\boldsymbol{x}, \boldsymbol{y}, \boldsymbol{z})$ forms the global coordinate. θ_p and θ_q are the angle from $\boldsymbol{x}$ to $\boldsymbol{p}$ and $\boldsymbol{q}$, respectively.

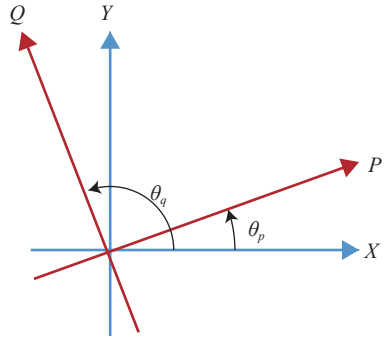

Figure 3 Diagram of $\boldsymbol{p}$ and $\boldsymbol{q}$ in the XOY coordinates and the POQ coordinates.

Obversely, we have

$$\begin{aligned}\boldsymbol{p} &= \boldsymbol{x}\cos\theta_p + \boldsymbol{y}\sin\theta_p\\ \boldsymbol{q} &= \boldsymbol{x}\cos\theta_q + \boldsymbol{y}\sin\theta_q\end{aligned}$$

and

$$\theta_q = \theta_p + \pi/2$$

According to the trigonometric function and complex variable function knowledge, it can be obtained that

$$\begin{aligned}\mathbf{rot}(\theta) &= \mathbf{rot}((\theta - \theta_p) + \theta_p)\\ &= \cos(\theta - \theta_p)\mathbf{rot}\theta_p + \sin(\theta - \theta_p)\mathbf{rot}(\theta_p + \pi/2)\\ &= \cos(\theta - \theta_p)\mathbf{rot}\theta_p + \sin(\theta - \theta_p)\mathbf{rot}\theta_q\end{aligned} \tag{5}$$

The polarization vector $\mathbf{rot}\theta$ is decomposed into two polarization vectors, $\mathbf{rot}\theta_p$ and $\mathbf{rot}\theta_q$. The orthogonal relationship between $\mathbf{rot}\theta_p$ and $\mathbf{rot}\theta_q$ can be proved by making inner product that

$$\mathbf{rot}\theta_p \cdot (\mathbf{rot}\theta_q)^* = 0$$

By substituting (5) into (4) and referring to Figure 2, the decomposed results are equivalent to that of the direct decomposition of the wave expression.

4. Discrete sequences of the polarization control operator

Inspired by digital signal processing approaches, discrete sequences of length N in the spatial polarization domain can be constructed and expressed as

$$\{\boldsymbol{S}(k)\} = \left\{\mathbf{rot}\left(\frac{2\pi k}{N}\right)\right\}(k = 0, 1, \ldots, N-1) \quad (6)$$

According to the properties of the polarization operator, items in equation (6) can be divided into three categories. For $k \in (0, N/4) \cup (N/2, 3N/4)$, the sequence item stands for a right-handed polarized wave. For $k \in (N/4, N/2) \cup (3N/4, N)$, the sequence item stands for a left-handed polarized wave. And for $k \in \{0, N/4, N/2, 3N/4\}$, the sequence item stands for a linearly polarized wave.

Items in $\{\boldsymbol{S}(k)\}$ can be used as bases to expand electromagnetic waves, expressed as

$$\boldsymbol{E} = \mathrm{Re}\left[\mathrm{e}^{\mathrm{j}(\omega t - g_u)} \sum_{k=0}^{N-1} A_k \mathbf{rot}\left(\frac{2\pi k}{N}\right)\right] \quad (7)$$

The implications of (7) is that the **rot**[ ] items constitute the polarization spectrum of the electromagnetic wave, where A_k is the amplitude of the k-th spectrum line. For illustrative purposes, Figure 4 gives the diagram of a discrete decomposition of an electromagnetic wave.

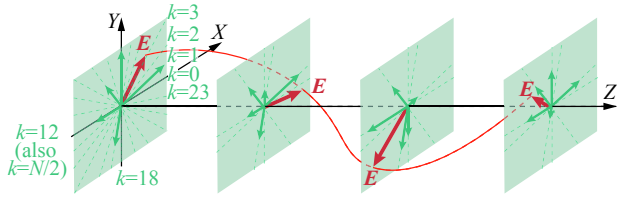

Figure 4 The discrete decomposition format of the electromagnetic wave by 24 polarization basis in the XYZ coordinates.

A pair of transform formulas can be constructed referring to discrete Fourier transform and inverse discrete Fourier transform, expressed as

$$\tilde{E}[k] = \sum_{n=0}^{N-1} \tilde{e}[n] \cdot P_N^{kn}$$

$$\tilde{e}[n] = \frac{1}{N} \sum_{k=0}^{N-1} \tilde{E}[k] \cdot P_N^{-kn}$$

where $P_N^{kn} = \mathbf{rot}(2\pi kn/N)$, $P_N^{-kn} = \mathbf{rot}(-2\pi kn/N)$.

III. Simulation Results of Polarization Control over Electromagnetic Wave

This section considers controlling the electromagnetic waves through the proposed polarization control operator with a fixed angle parameter and a time-varying angle parameter. These examples show that the polarization control operator can achieve complex control over the rotation and amplitude of the field.

1. Polarization control operator with fixed α

A left-handed circularly polarized plane wave traveling in the $\boldsymbol{z}$ direction in the $(\boldsymbol{x}, \boldsymbol{y}, \boldsymbol{z})$ coordinate frame is given as

$$\boldsymbol{E} = E_0 \mathrm{Re}[\mathrm{e}^{\mathrm{j}(\omega t - kz)} \mathbf{rot}\alpha]\,|_{\alpha=\frac{\pi}{4}} \quad (8)$$

where E_0 is the amplitude of the electromagnetic wave.

When α in (8) is set to another fixed value at $z = 0$, the wave propagating from $z = 0$ is expressed as

$$\boldsymbol{E}_{\mathrm{rot}} = E_0 \mathrm{Re}[\mathrm{e}^{\mathrm{j}(\omega t - kz)} \mathbf{rot}\alpha]$$

The influences introduced by $\mathbf{rot}\alpha$ are reflected in the scaling of the $\boldsymbol{E}_x$ component and $\boldsymbol{E}_y$ component by $\cos\alpha$ and $\sin\alpha$ times respectively. Therefore, $\boldsymbol{E}_{\mathrm{rot}}$ can have a different polarization state than $\boldsymbol{E}$. In addition, since α is a real constant independent of time and distance, the polarization state of $\boldsymbol{E}_{\mathrm{rot}}$ is steady.

Figure 5 shows the rotation of $\boldsymbol{E}_{\mathrm{rot}}$ with time and distance for different fixed α values. The black arrays are the field vectors and the red curve is the path of the field vector tip. When $\alpha = \pi/6$, the electromagnetic wave is noted as $\boldsymbol{E}_{\mathrm{rot1}}$. When $\alpha = 2\pi/3$, the electromagnetic wave is noted as $\boldsymbol{E}_{\mathrm{rot2}}$. Both of $\boldsymbol{E}_{\mathrm{rot1}}$ and $\boldsymbol{E}_{\mathrm{rot2}}$ have different constant polarization state than $\boldsymbol{E}$. Specifically, the polarization ellipses of $\boldsymbol{E}_{\mathrm{rot1}}$ and $\boldsymbol{E}_{\mathrm{rot2}}$ have the same axis ratio of $\sqrt{3}$. However, $\boldsymbol{E}_{\mathrm{rot1}}$ is left-handed and $\boldsymbol{E}_{\mathrm{rot2}}$ is right-handed.

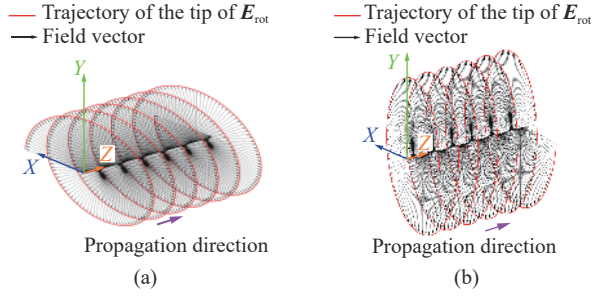

Figure 5 Rotation of $\boldsymbol{E}_{\mathrm{rot}}$ with time and distance for different fixed α values in the XYZ coordinates. (a) $\alpha = \pi/6$; (b) $\alpha = 2\pi/3$.

The simulation results are consistent with the demonstration in Section II.2. By controlling α to take different values, different steadily polarized electromagnetic waves can be obtained.

2. Polarization control operator with continuously time-varying α

Without loss of generality, this subsection discusses the case that α varies uniformly over time. The value of α is expressed as

$$\alpha(t) = \omega_p t$$

where ω_p is the angular frequency of α over time. When α in (8) is set to the time-varying value at $z = z_0$, the wave propagating from z_0 is expressed as

$$\boldsymbol{E}_{\mathrm{rot}} = E_0 \mathrm{Re}\left(\mathrm{e}^{\mathrm{j}(\omega t - kz)} \mathbf{rot}\left(\omega_p\left(t - \frac{z - z_0}{c_0}\right)\right)\right)$$

In contrast to the results in which α is constant, the scaling introduced by $\mathbf{rot}\alpha(t)$ on $\boldsymbol{E}_x$ and $\boldsymbol{E}_y$ is time-varying, which makes the polarization state of the wave change over time. This can lead to complex waveforms. Since the value of ω_p decides the changing rate of the polarization state and the value of ω decides the rotation rate of the field vector, the waveforms controlled by continuously time-varying polarization control operator are specifically discussed with the relative value of ω and ω_p. In the following discussion, z_0 is set to 0.

When $\omega_p < \omega$, the period of $\boldsymbol{E}_{\text{rot}}$ is extended to $T_{\text{rot}} = 2\pi/\omega_p$. Compared to the original wave of $\boldsymbol{E}$, the new wave of $\boldsymbol{E}_{\text{rot}}$ controlled by $\mathbf{rot}\alpha(t)$ presents a new wave packet. The minimum distance of the repeated wave packet, which is noted by λ_p, is larger than the wavelength of the electromagnetic wave.

Figure 6 shows the polarization patterns with different ω_p by plotting the electric field vectors at different locations and connecting the tips of the vectors. The waves are observed over $\Delta z = 30\lambda$. In Figures 6(a), (c) and (e), the field paths are projected onto the XOY plane. In Figures 6(b), (d) and (f), the field paths are presented as the waveforms propagating with time and distance. It is noted that the densely displayed field vectors form the black blocks in the waveform figures. As shown in Figure 6, with the decrease of ω_p, λ_p is getting longer and the projection traces are getting denser.

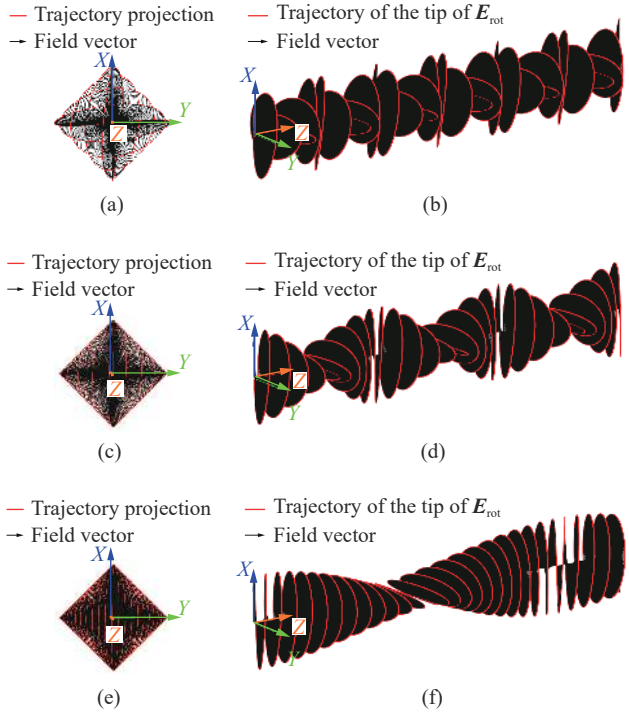

Figure 6 Polarization pattern for different ω_p values. (a) Field path projection on the XOY plane, $\omega_p = \omega/10$; (b) Waveform, $\omega_p = \omega/10$; (c) Field path projection on the XOY plane, $\omega_p = \omega/20$; (d) Waveform, $\omega_p = \omega/20$; (e) Field path projection on the XOY plane, $\omega_p = \omega/50$; (f) Waveform, $\omega_p = \omega/50$.

To analyze the characteristics of the waveforms in detail, cross sections from different viewing angles are observed for $\omega_p = \omega/20$. The observation configuration is shown in Figure 7. The cross sections with different viewing angles are shown in Figure 8. The waves are observed over $\Delta z = 20\lambda$. It can be found that the cross section shows a modulation effect. The modulation parameters are different for different θ angles. This indicates that the proposed polarization control operator can be utilized to achieve modulation in the angular domain.

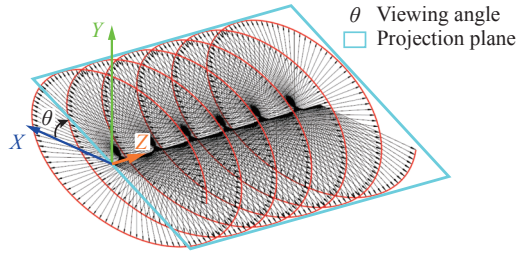

Figure 7 Definition of viewing angles in the XYZ coordinates.

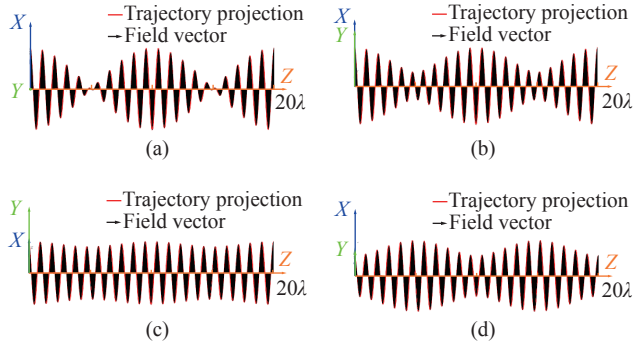

Figure 8 Cross sections from different viewing angles in the XYZ coordinates. (a) $\theta = 0$; (b) $\theta = \pi/9$; (c) $\theta = 4\pi/9$; (d) $\theta = 2\pi/3$.

When $\omega_p = \omega$, the scaling introduced by $\mathbf{rot}\alpha(t)$ on the field components has the same angular frequency with the electromagnetic wave. Therefore, the period of $\boldsymbol{E}_{\text{rot}}$ is the half of that of $\boldsymbol{E}$, which is $T_{\text{rot}} = \pi/\omega$. The x component and the y component of $\boldsymbol{E}_{\text{rot}}$ satisfy the line equation given by

$$E_{\text{rot},x} = E_0 + E_{\text{rot},y}$$

The field path projection onto the XOY plane and the waveform propagating with time and distance are shown in Figure 9. The waves are observed over $\Delta z = 4\lambda$. A linearly polarized wave of a new polarized

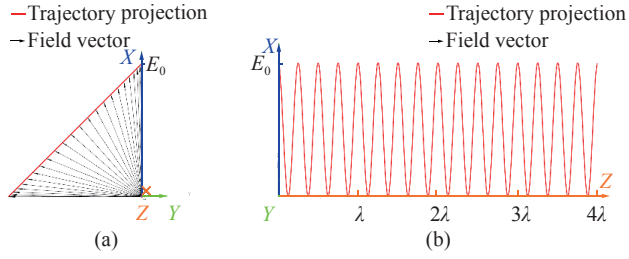

Figure 9 Polarization pattern when $\omega_p = \omega$. (a) Field path projection on the XOY plane; (b) Field path projection on the XOZ plane.

direction is attained.

When $\omega_p > \omega$, the polarization state of the wave is changed more frequently. Figure 10 shows the projection of $\boldsymbol{E}_{\text{rot}}$ on the XOY plane. The projection patterns here are more convex compared to that of $\omega_p < \omega$. Also, with the increase of ω_p, λ_p is getting longer and the projection traces are getting denser, and the new wave contains a wider variety of polarization states.

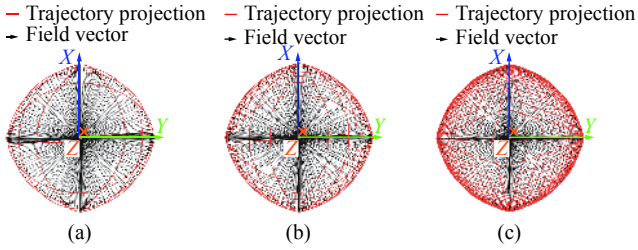

Figure 10 Field path projection on the XOY plane for different values of ω_p. (a) $\omega_p = 10\omega$; (b) $\omega_p = 20\omega$; (c) $\omega_p = 50\omega$.

Figure 11 shows the cross sections from different viewing angles when $\omega_p = 20\omega$. Similar modulation effects are observed in the angular domain when $\omega_p < \omega$.

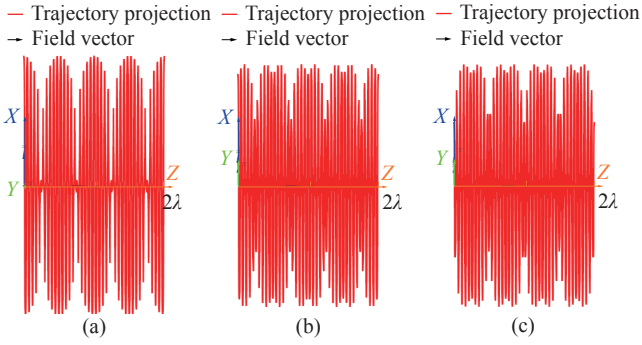

Figure 11 Cross sections from different viewing angles in the XYZ coordinates. (a) $\theta = 0$; (b) $\theta = \pi/6$; (c) $\theta = \pi/3$.

In summary, by adjusting the parameter of the proposed control polarization operator to change with time, the waveform of the electromagnetic wave in the angular domain can be modulated. This indicates a possibility that by designing the parameter of the proposed polarization control operator, the wave can be used to transmit multiple information simultaneously at different angles.

IV. Conclusion

A polarization control operator is proposed in this paper, which is proven to be able to describe the instantaneous states and control the polarization state of the electromagnetic wave. Two typical simulation results are given about controlling the polarization state of a left-handed circularly polarized electromagnetic wave. When the operator is applied to a fixed parameter, the electromagnetic wave can be controlled as different constant polarization waves. When the operator is applied to a parameter varying with time, the electromagnetic wave with different modulation characteristics at different angles can be obtained. Through these applications, it can be found that the proposed polarization control operator can control the polarization properties of electromagnetic waves.

In further work, we will continue to use the polarization control operator for more applications in the field of electromagnetic compatibility.

Appendix A

The basic properties and operation rules of the polarization control operator are derived based on the trigonometric function and complex variable function knowledge, as shown in Tables A-1 and A-2.

Table A-1 Basic properties of the polarization operator

No.	Transformation	Result
1	$\lvert\mathbf{rot}\theta\rvert$	1
2	$\mathbf{rot}(-\theta)$	$\text{conj}(\mathbf{rot}\theta)$
3	$\boldsymbol{w}\cdot\mathbf{rot}\theta$	0
4	$\text{Re}(\mathbf{rot}\theta)$	$\boldsymbol{u}\cos\theta$
5	$\text{Im}(\mathbf{rot}\theta)$	$\boldsymbol{v}\sin\theta$
6	$\text{conj}(\mathbf{rot}\theta)$	$\mathbf{rot}(-\theta)$
7	$\mathbf{rot}0$	$\boldsymbol{u}$
8	$\mathbf{rot}(\pi/4)$	$\sqrt{2}\,(\boldsymbol{u}+\text{j}\boldsymbol{v})\,/2$
9	$\mathbf{rot}(\pi/2)$	$\text{j}\boldsymbol{v}$

Table A-2 Operation rules of the polarization operator

No.	Transformation	Result
1	$\mathbf{rot}(\theta_1+\theta_2)$	$\cos\theta_1\mathbf{rot}\theta_2+\sin\theta_1\mathbf{rot}(\theta_2+\pi/2)$
2	$\mathbf{rot}(\theta+\pi/2)$	$\text{j}\boldsymbol{w}\times\mathbf{rot}(-\theta)$
3	$\mathbf{rot}(\theta+k\pi)$	$(-1)^k\mathbf{rot}\theta$
4	$\mathbf{rot}\theta_1\times\mathbf{rot}\theta_2$	$-\text{j}\boldsymbol{w}\sin(\theta_1-\theta_2)$
5	$\mathbf{rot}\theta_1\cdot\mathbf{rot}\theta_2$	$\cos(\theta_1+\theta_2)$
6	$\mathbf{rot}\theta_1+\mathbf{rot}\theta_2$	$2\mathbf{rot}[(\theta_1+\theta_2)/2]\cos[(\theta_1-\theta_2)/2]$
7	$\text{d}(\mathbf{rot}\theta)/\text{d}\theta$	$\mathbf{rot}(\theta+\pi/2)$
8	$\text{d}^2(\mathbf{rot}\theta)/\text{d}\theta^2$	$-\mathbf{rot}\theta$

References

[1] L. H. Pang, J. Zhang, Y. Zhang, *et al.*, "Investigation and comparison of 5G channel models: From QuaDRiGa, NYUSIM, and MG5G perspectives," *Chinese Journal of Electronics*, vol. 31, no. 1, pp. 1–17, 2022.

[2] H. Huang, Y. Liu, and S. X. Gong, "Broadband dual-polarized omnidirectional antenna for 2G/3G/LTE/WiFi applications," *IEEE Antennas and Wireless Propagation Letters*, vol. 15, pp. 576–579, 2016.

[3] F. Yildirim, A. S. Sadri, and H. P. Liu, "Polarization effects for indoor wireless communications at 60 GHz," *IEEE Communications Letters*, vol. 12, no. 9, pp. 660–662, 2008.

[4] X. S. Wang, Y. Z. Li, H. Y. Dai, *et al.*, "Research on instantaneous polarization radar system and external experiment," *Chinese Science Bulletin*, vol. 55, no. 15, pp. 1560–1567,

2010.
[5] L. F. Shi, X. S. Wang, and S. P. Xiao, "Polarization discrimination between repeater false-target and radar target," *Science in China Series F:Information Sciences*, vol. 52, no. 1, pp. 149–158, 2009.
[6] H. Mott, *Polarization in Antennas and Radar*. John Wiley & Sons, New York, NY, USA, pp. 54–108, 1986.
[7] R. C. Jones, "A new calculus for the treatment of optical systems I. Description and discussion of the calculus," *Journal of the Optical Society of America*, vol. 31, no. 7, pp. 488–493, 1941.
[8] Z. C. Yang and K. F. Warnick, "Analysis and design of intrinsically dual circular polarized microstrip antennas using an equivalent circuit model and Jones matrix formulation," *IEEE Transactions on Antennas and Propagation*, vol. 64, no. 9, pp. 3858–3868, 2016.
[9] I. Moreno, M. J. Yzuel, J. Campos, *et al.*, "Jones matrix treatment for polarization Fourier optics," *Journal of Modern Optics*, vol. 51, no. 14, pp. 2031–2038, 2004.
[10] G. G. Stokes, *On the Theories of the Internal Friction of Fluids in Motion, and of the Equilibrium and Motion of Elastic Solids*. Cambridge University Press, Cambridge, pp. 75–129, 2009.
[11] M. Born and E. Wolf, *Principles of Optics*: *Electromagnetic Theory of Propagation, Interference and Diffraction of Light*, 6th ed., Pergamon Press, Oxford, UK, pp. 23–36, 1980.
[12] G. Milione, H. I. Sztul, D. A. Nolan, *et al.*, "Higher-order Poincaré sphere, Stokes parameters, and the angular momentum of light," *Physical Review Letters*, vol. 107, no. 5, article no. 053601, 2011.
[13] G. A. Deschamps and P. Mast, "Poincaré sphere representation of partially polarized fields," *IEEE Transactions on Antennas and Propagation*, vol. 21, no. 4, pp. 474–478, 1973.
[14] H. Jiang, Y. Yao, T. Xiu, *et al.*, "High-gain dual circularly polarized antenna for air-to-ground wireless link," *Chinese Journal of Electronics*, vol. 31, no. 3, pp. 555–561, 2022.
[15] X. Gao, X. Han, W. P. Cao, *et al.*, "Ultrawideband and high-efficiency linear polarization converter based on double v-shaped metasurface," *IEEE Transactions on Antennas and Propagation*, vol. 63, no. 8, pp. 3522–3530, 2015.
[16] Z. Ul Abidin, P. Xiao, M. Amin, *et al.*, "Circular polarization modulation for digital communication systems," in *Proceedings of the 8th International Symposium on Communication Systems, Networks & Digital Signal Processing*, Poznan, Poland, pp. 1–6, 2012.
[17] S. H. Doan, S. C. Kwon, and H. G. Yeh, "Achievable capacity of multipolarization MIMO with the practical polarization-agile antennas," *IEEE Systems Journal*, vol. 15, no. 2, pp. 3081–3092, 2021.
[18] J. L. Zhang, K. J. Kim, A. A. Glazunov, *et al.*, "Generalized polarization-space modulation," *IEEE Transactions on Communications*, vol. 68, no. 1, pp. 258–273, 2020.
[19] A. Al-Wahhamy, H. Al-Rizzo, and N. E. Buris, "Efficient evaluation of massive MIMO channel capacity," *IEEE Systems Journal*, vol. 14, no. 1, pp. 614–620, 2020.
[20] G. W. Yang, J. Y. Li, B. Cao, *et al.*, "A compact reconfigurable microstrip antenna with multidirectional beam and multipolarization," *IEEE Transactions on Antennas and Propagation*, vol. 67, no. 2, pp. 1358–1363, 2019.
[21] D. Yang, Y. Xi, H. Q. Zhai, *et al.*, "High-gain polarization reconfigurable antenna applied to 5G communication frequency band," in *Proceedings of the 2020 International Conference on Microwave and Millimeter Wave Technology*, Shanghai, China, pp. 1–3, 2020.
[22] D. D. Liu, L. Q. Gui, K. Chen, *et al.*, "Theoretical analysis and comparison of OAM waves generated by three kinds of antenna array," *Digital Communications and Networks*, vol. 7, no. 1, pp. 16–28, 2021.
[23] X. W. Xiong, S. L. Zheng, Z. L. Zhu, *et al.*, "Experimental study of plane spiral OAM mode-group based MIMO communications," *IEEE Transactions on Antennas and Propagation*, vol. 70, no. 1, pp. 641–653, 2022.
[24] C. Xu, S. L. Zheng, W. T. Zhang, *et al.*, "Free-space radio communication employing OAM multiplexing based on Rotman lens," *IEEE Microwave and Wireless Components Letters*, vol. 26, no. 9, pp. 738–740, 2016.
[25] D. L. Su, A. X. Chen, S. G. Xie, *et al.*, *Electromagnetic Field and Electromagnetic Wave*. Higher Education Press, Beijing, China, pp. 356–357, 2009. (in Chinese)

Shuo CUI was born in Hebei Province, China. She received the B.E. degree in applied physics from Beihang University, Beijing, China. She is currently a Ph.D. candidate of the School of Electronic and Information Engineering, Beihang University, Beijing, China. Her currently research interests include computational electromagnetics and electromagnetic environment.
(Email: cuishuo@buaa.edu.cn)

Yaoyao LI received the Ph.D. degree in electromagnetic compatibility and electromagnetic environment from Beihang University, Beijing, China, in 2017, where he is currently an Associate Professor in electronic science and technology. His current research interests include electromagnetic compatibility and computational electromagnetics.
(Email: liyaoyao@buaa.edu.cn)

Shijian ZHANG was born in Liaoning Province, China. He received the B.E. degree from Air Force Radar Academy, Wuhan, China. He is currently working toward the M.S. degree at Beihang University, Beijing, China. His research interests include electromagnetic scattering measurements and electromagnetic compatibility.
(Email: zsjhappy6058@163.com)

Ling CHEN was born in Zhejiang Province, China. She received the B.E. degree in measurement and control technology and instrument from China Jiliang University, Hangzhou, China. She is an M.S. candidate of Beihang University, Beijing, China. Her research interests include instrumentation and control equipments and electromagnetic compatibility.
(Email: zy2143209@buaa.edu.cn)

Cheng CAO was born in Hubei Province, China. He received the B.E. degree in electronic information engineering from Nanjing University of Aeronautics and Astronautics, Nanjing, China, and the Ph.D. degree in circuit and system from Beihang University, Beijing, China. His research interests includes system level electromagnetic compatibility and electromagnetic calculation software.
(Email: caocheng8230@buaa.edu.cn)

Donglin SU received the B.S., M.S., and Ph.D. degrees in electrical engineering from Beihang University (BUAA), Beijing, China, in 1983, 1986, and 1999, respectively. In 1986, she joined the School of Electronics and Information Engineering, BUAA, where she was first an Assistant, then a Lecturer, later on an Associate Professor, and is currently a Full Professor. From 1996 to 1998, she was a Visiting Scholar with the Department of Electrical Engineering, University of California, Los Angeles, Los Angeles, CA, USA, under the BUAA-UCLA Joint Ph.D. Program. She has authored more than 100 papers and coauthored several books. Her research interests include the numerical methods for microwave and millimeterwave integrated circuits and systematic electromagnetic compatibility design of various aircrafts. Dr. Su is a Member of the Chinese Academy of Engineering. She is a Fellow of the Chinese Institute of Electronics. She is the Chair of Beijing Chapter of the IEEE Antennas and Propagation Society and the Deputy Chair of the Antennas Society, Chinese Institute of Electronics. She was the recipient of the National Science and Technology Advancement Award of China in 2007 and 2012, and the National Technology Invention Award of China in 2018.

(Email: sdl@buaa.edu.cn)